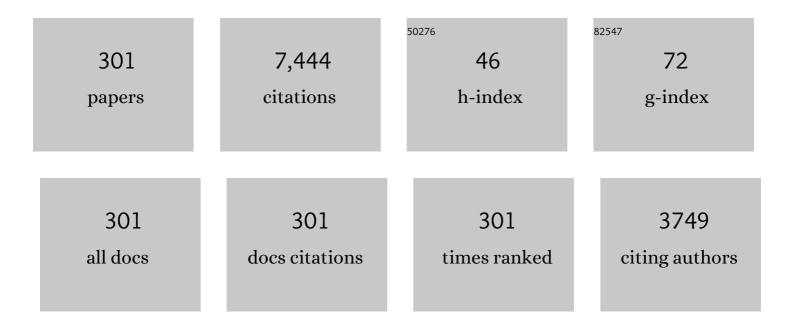
Yiping Wang

List of Publications by Year in descending order

Source: https://exaly.com/author-pdf/6095153/publications.pdf Version: 2024-02-01



#	Article	IF	CITATIONS
1	Fusion Splicing Photonic Crystal Fibers and Conventional Single-Mode Fibers: Microhole Collapse Effect. Journal of Lightwave Technology, 2007, 25, 3563-3574.	4.6	236
2	Sub-micron silica diaphragm-based fiber-tip Fabry–Perot interferometer for pressure measurement. Optics Letters, 2014, 39, 2827.	3.3	190
3	Review of long period fiber gratings written by CO2 laser. Journal of Applied Physics, 2010, 108, .	2.5	187
4	Surface plasmon resonance refractive sensor based on silver-coated side-polished fiber. Sensors and Actuators B: Chemical, 2016, 230, 206-211.	7.8	181
5	High-sensitivity strain sensor based on in-fiber improved Fabry–Perot interferometer. Optics Letters, 2014, 39, 2121.	3.3	180
6	Surface plasmon resonance biosensor based on gold-coated side-polished hexagonal structure photonic crystal fiber. Optics Express, 2017, 25, 20313.	3.4	172
7	Intensity modulated refractive index sensor based on optical fiber Michelson interferometer. Sensors and Actuators B: Chemical, 2015, 208, 315-319.	7.8	154
8	Simultaneous measurement of pressure and temperature by employing Fabry-Perot interferometer based on pendant polymer droplet. Optics Express, 2015, 23, 1906.	3.4	138
9	Simultaneous measurement of strain and temperature by employing fiber Mach-Zehnder interferometer. Optics Express, 2014, 22, 1680.	3.4	127
10	Long period gratings in air-core photonic bandgap fibers. Optics Express, 2008, 16, 2784.	3.4	126
11	Highly-sensitive gas pressure sensor using twin-core fiber based in-line Mach-Zehnder interferometer. Optics Express, 2015, 23, 6673.	3.4	121
12	Highly sensitive surface plasmon resonance biosensor based on a low-index polymer optical fiber. Optics Express, 2018, 26, 3988.	3.4	106
13	High-sensitivity strain sensor based on in-fiber rectangular air bubble. Scientific Reports, 2015, 5, 7624.	3.3	100
14	Antiresonant reflecting guidance mechanism in hollow-core fiber for gas pressure sensing. Optics Express, 2016, 24, 27890.	3.4	98
15	Orbital Angular Momentum Mode Converter Based on Helical Long Period Fiber Grating Inscribed by Hydrogen–Oxygen Flame. Journal of Lightwave Technology, 2018, 36, 1683-1688.	4.6	92
16	Intensity measurement bend sensors based on periodically tapered soft glass fibers. Optics Letters, 2011, 36, 558.	3.3	87
17	Two-dimensional vector bending sensor based on seven-core fiber Bragg gratings. Optics Express, 2018, 26, 23770.	3.4	86
18	Asymmetrical in-fiber Mach-Zehnder interferometer for curvature measurement. Optics Express, 2015, 23, 14596.	3.4	82

#	Article	IF	CITATIONS
19	Label-free detection of bovine serum albumin based on an in-fiber Mach-Zehnder interferometric biosensor. Optics Express, 2017, 25, 17105.	3.4	82
20	Temperature-insensitive refractive index sensor based on in-fiber Michelson interferometer. Sensors and Actuators B: Chemical, 2014, 199, 31-35.	7.8	80
21	Review of Femtosecond-Laser-Inscribed Fiber Bragg Gratings: Fabrication Technologies and Sensing Applications. Photonic Sensors, 2021, 11, 203-226.	5.0	78
22	Ultrasensitive magnetic field sensor based on an in-fiber Mach–Zehnder interferometer with a magnetic fluid component. Photonics Research, 2016, 4, 197.	7.0	76
23	Ultrasensitive refractive index sensor based on a Mach–Zehnder interferometer created in twin-core fiber. Optics Letters, 2014, 39, 4982.	3.3	72
24	High-order orbital angular momentum mode generator based on twisted photonic crystal fiber. Optics Letters, 2018, 43, 1786.	3.3	71
25	Torsion, Refractive Index, and Temperature Sensors Based on An Improved Helical Long Period Fiber Grating. Journal of Lightwave Technology, 2020, 38, 2504-2510.	4.6	71
26	High-Sensitivity Gas-Pressure Sensor Based on Fiber-Tip PVC Diaphragm Fabry–Pérot Interferometer. Journal of Lightwave Technology, 2017, 35, 4067-4071.	4.6	70
27	Measurement of high pressure and high temperature using a dual-cavity Fabry–Perot interferometer created in cascade hollow-core fibers. Optics Letters, 2018, 43, 6009.	3.3	70
28	Femtosecond Laser Inscription of Fiber Bragg Grating in Twin-Core Few-Mode Fiber for Directional Bend Sensing. Journal of Lightwave Technology, 2017, 35, 4670-4676.	4.6	69
29	Temperature-insensitivity gas pressure sensor based on inflated long period fiber grating inscribed in photonic crystal fiber. Optics Letters, 2015, 40, 1791.	3.3	66
30	In-fiber polarizer based on a long-period fiber grating written on photonic crystal fiber. Optics Letters, 2007, 32, 1035.	3.3	64
31	Towards high sensitivity gas detection with hollow-core photonic bandgap fibers. Optics Express, 2014, 22, 24894.	3.4	64
32	High-sensitivity strain sensor based on inflated long period fiber grating. Optics Letters, 2014, 39, 5463.	3.3	63
33	Long period fiber grating based on periodically screw-type distortions for torsion sensing. Optics Express, 2017, 25, 14308.	3.4	63
34	An Optoelectronic Oscillator for High Sensitivity Temperature Sensing. IEEE Photonics Technology Letters, 2016, 28, 1458-1461.	2.5	62
35	Fiber-tip polymer clamped-beam probe for high-sensitivity nanoforce measurements. Light: Science and Applications, 2021, 10, 171.	16.6	61
36	Temperature-controlled transformation in fiber types of fluid-filled photonic crystal fibers and applications. Optics Letters, 2010, 35, 88.	3.3	59

#	Article	IF	CITATIONS
37	Splicing Ge-doped photonic crystal fibers using commercial fusion splicer with default discharge parameters. Optics Express, 2008, 16, 7258.	3.4	58
38	Tunable Electro-Optical Modulator Based on a Photonic Crystal Fiber Selectively Filled With Liquid Crystal. Journal of Lightwave Technology, 2019, 37, 1903-1908.	4.6	56
39	Sapphire fiber Bragg gratings inscribed with a femtosecond laser line-by-line scanning technique. Optics Letters, 2018, 43, 4562.	3.3	55
40	Long Period Fiber Gratings Inscribed by Periodically Tapering a Fiber. IEEE Photonics Technology Letters, 2014, 26, 698-701.	2.5	54
41	Highly sensitive temperature sensor based on a polymer-infiltrated Mach–Zehnder interferometer created in graded index fiber. Optics Letters, 2019, 44, 2466.	3.3	53
42	Automatic Arc Discharge-Induced Helical Long Period Fiber Gratings and Its Sensing Applications. IEEE Photonics Technology Letters, 2017, 29, 873-876.	2.5	50
43	Nano silica diaphragm in-fiber cavity for gas pressure measurement. Scientific Reports, 2017, 7, 787.	3.3	50
44	Liquid modified photonic crystal fiber for simultaneous temperature and strain measurement. Photonics Research, 2017, 5, 129.	7.0	50
45	Sensing properties of fiber Bragg gratings in small-core Ge-doped photonic crystal fibers. Optics Communications, 2009, 282, 1129-1134.	2.1	49
46	Optical switch based on a fluid-filled photonic crystal fiber Bragg grating. Optics Letters, 2009, 34, 3683.	3.3	47
47	Polarization-independent orbital angular momentum generator based on a chiral fiber grating. Optics Letters, 2019, 44, 61.	3.3	47
48	D-shaped fiber grating refractive index sensor induced by an ultrashort pulse laser. Applied Optics, 2016, 55, 1525.	2.1	46
49	Femtosecond laser point-by-point inscription of an ultra-weak fiber Bragg grating array for distributed high-temperature sensing. Optics Express, 2021, 29, 32615.	3.4	45
50	Tunable phase-shifted fiber Bragg grating based on femtosecond laser fabricated in-grating bubble. Optics Letters, 2013, 38, 4473.	3.3	44
51	Femtosecond laser-inscribed fiber interface Mach–Zehnder interferometer for temperature-insensitive refractive index measurement. Optics Letters, 2018, 43, 4421.	3.3	43
52	Comparison of Linear- and Star-Shaped Fused-Ring Electron Acceptors. , 2019, 1, 367-374.		43
53	Electrically Tunable Four-Wave-Mixing in Graphene Heterogeneous Fiber for Individual Gas Molecule Detection. Nano Letters, 2020, 20, 6473-6480.	9.1	42
54	Highly birefringent phase-shifted fiber Bragg gratings inscribed with femtosecond laser. Optics Letters, 2015, 40, 2008.	3.3	41

#	Article	IF	CITATIONS
55	Diaphragm-free gas-pressure sensor probe based on hollow-core photonic bandgap fiber. Optics Letters, 2018, 43, 3017.	3.3	40
56	High-Performance Mid-Bandgap Fused-Pyrene Electron Acceptor. Chemistry of Materials, 2019, 31, 6484-6490.	6.7	40
57	Negative-index gratings formed by femtosecond laser overexposure and thermal regeneration. Scientific Reports, 2016, 6, 23379.	3.3	39
58	Fiber surface Bragg grating waveguide for refractive index measurements. Optics Letters, 2017, 42, 1684.	3.3	39
59	Selective fiber Bragg grating inscription in four-core fiber for two-dimension vector bending sensing. Optics Express, 2020, 28, 26461.	3.4	39
60	Simultaneous Refractive Index and Temperature Measurement With LPFG and Liquid-Filled PCF. IEEE Photonics Technology Letters, 2015, 27, 375-378.	2.5	38
61	Optofluidic gutter oil discrimination based on a hybrid-waveguide coupler in fibre. Lab on A Chip, 2018, 18, 595-600.	6.0	37
62	Mechanism and Characteristics of Humidity Sensing with Polyvinyl Alcohol-Coated Fiber Surface Plasmon Resonance Sensor. Sensors, 2018, 18, 2029.	3.8	35
63	Fiber Bragg grating inscription in pure-silica and Ge-doped photonic crystal fibers. Applied Optics, 2009, 48, 1963.	2.1	34
64	Coupled Local-Mode Theory for Strongly Modulated Long Period Gratings. Journal of Lightwave Technology, 2010, 28, 1745-1751.	4.6	34
65	Compact tunable multibandpass filters based on liquid-filled photonic crystal fibers. Optics Letters, 2014, 39, 2148.	3.3	34
66	Parallel-Integrated Fiber Bragg Gratings Inscribed by Femtosecond Laser Point-by-Point Technology. Journal of Lightwave Technology, 2019, 37, 2185-2193.	4.6	34
67	Residual-stress-induced helical long period fiber gratings for sensing applications. Optics Express, 2018, 26, 24114.	3.4	34
68	Fiber optic hydrogen sensor based on a Fabry–Perot interferometer with a fiber Bragg grating and a nanofilm. Lab on A Chip, 2021, 21, 1752-1758.	6.0	33
69	Generation and detection of broadband multi-channel orbital angular momentum by micrometer-scale meta-reflectarray. Optics Express, 2016, 24, 212.	3.4	32
70	Fiber-Tip Polymer Microcantilever for Fast and Highly Sensitive Hydrogen Measurement. ACS Applied Materials & Interfaces, 2020, 12, 33163-33172.	8.0	32
71	Transverse-load, strain, temperature, and torsion sensors based on a helical photonic crystal fiber. Optics Letters, 2019, 44, 1984.	3.3	32
72	Femtosecond laser microprinting of a polymer fiber Bragg grating for high-sensitivity temperature measurements. Optics Letters, 2018, 43, 3409.	3.3	31

#	Article	IF	CITATIONS
73	Surface plasmon resonance refractive index sensor based on fiber-interface waveguide inscribed by femtosecond laser. Optics Letters, 2019, 44, 2434.	3.3	31
74	Review of Optical Humidity Sensors. Sensors, 2021, 21, 8049.	3.8	31
75	High-sensitivity gas pressure sensor based on hollow-core photonic bandgap fiber Mach-Zehnder interferometer. Optics Express, 2018, 26, 30108.	3.4	30
76	Femtosecond-laser-inscribed sampled fiber Bragg grating with ultrahigh thermal stability. Optics Express, 2016, 24, 3981.	3.4	29
77	Optical Fiber Bragg Grating Pressure Sensor Based on Dual-Frequency Optoelectronic Oscillator. IEEE Photonics Technology Letters, 2017, 29, 1864-1867.	2.5	29
78	High-Sensitivity Temperature Sensor Based on Polarization Maintaining Fiber Sagnac Loop. Photonic Sensors, 2019, 9, 25-32.	5.0	29
79	Intensity-Modulated Strain Sensor Based on Fiber In-Line Mach–Zehnder Interferometer. IEEE Photonics Technology Letters, 2014, 26, 508-511.	2.5	28
80	Simultaneous Measurement of Strain and Temperature by a Sawtooth Stressor-Assisted Highly Birefringent Fiber Bragg Grating. Journal of Lightwave Technology, 2020, 38, 2060-2066.	4.6	28
81	Multi-layer, offset-coupled sapphire fiber Bragg gratings for high-temperature measurements. Optics Letters, 2019, 44, 4211.	3.3	28
82	Improved bending property of half-filled photonic crystal fiber. Optics Express, 2010, 18, 12197.	3.4	27
83	High-Sensitivity Temperature Sensor Based on a Coated Single-Mode Fiber Loop. Journal of Lightwave Technology, 2015, 33, 4019-4026.	4.6	26
84	Resolution-Enhanced Fiber Grating Refractive Index Sensor Based on an Optoelectronic Oscillator. IEEE Sensors Journal, 2018, 18, 9562-9567.	4.7	26
85	A Miniature Fiber Collimator for Highly Sensitive Bend Measurements. Journal of Lightwave Technology, 2018, 36, 2827-2833.	4.6	26
86	Fused octacyclic electron acceptor isomers for organic solar cells. Journal of Materials Chemistry A, 2019, 7, 21432-21437.	10.3	26
87	Ultra-dense perfect optical orbital angular momentum multiplexed holography. Optics Express, 2021, 29, 28452.	3.4	26
88	Femtosecond laser auto-positioning direct writing of a multicore fiber Bragg grating array for shape sensing. Optics Letters, 2022, 47, 758.	3.3	25
89	Automatic arc discharge technology for inscribing long period fiber gratings. Applied Optics, 2016, 55, 3873.	2.1	24
90	Torsion Sensor with Rotation Direction Discrimination Based on a Pre-twisted In-Fiber Mach–Zehnder Interferometer. IEEE Photonics Journal, 2017, 9, 1-8.	2.0	24

#	Article	IF	CITATIONS
91	Efficient point-by-point Bragg grating inscription in sapphire fiber using femtosecond laser filaments. Optics Letters, 2021, 46, 2742.	3.3	24
92	Phase-shifted fiber Bragg grating modulated by a hollow cavity for measuring gas pressure. Optics Letters, 2020, 45, 507.	3.3	24
93	Thermo-Optic Switching Effect Based on Fluid-Filled Photonic Crystal Fiber. IEEE Photonics Technology Letters, 2010, 22, 164-166.	2.5	23
94	Temperature Sensor Based on Side-Polished Fiber SPR Device Coated with Polymer. Sensors, 2019, 19, 4063.	3.8	23
95	Development of Polyhydroxyalkanoate-Based Polyurethane with Water-Thermal Response Shape-Memory Behavior as New 3D Elastomers Scaffolds. Polymers, 2019, 11, 1030.	4.5	23
96	In-Fiber Cascaded FPI Fabricated by Chemical-Assisted Femtosecond Laser Micromachining for Micro-Fluidic Sensing Applications. Journal of Lightwave Technology, 2019, 37, 3214-3221.	4.6	23
97	Magnetic field sensor based on helical long-period fiber grating with a three-core optical fiber. Optics Express, 2021, 29, 20649.	3.4	23
98	Thin-Core-Fiber-Based Long-Period Fiber Grating for High-Sensitivity Refractive Index Measurement. IEEE Photonics Journal, 2015, 7, 1-8.	2.0	22
99	Helical Microfiber Bragg Grating Printed by Femtosecond Laser for Refractive Index Sensing. IEEE Photonics Technology Letters, 2019, 31, 971-974.	2.5	22
100	Development of Nontoxic Biodegradable Polyurethanes Based on Polyhydroxyalkanoate and L-lysine Diisocyanate with Improved Mechanical Properties as New Elastomers Scaffolds. Polymers, 2019, 11, 1927.	4.5	22
101	Broadband tunable orbital angular momentum mode converter based on a conventional single-mode all-fiber configuration. Optics Express, 2021, 29, 15595.	3.4	22
102	High-Spatial-Resolution Strain Sensor Based on Distance Compensation and Image Wavelet Denoising Method in OFDR. Journal of Lightwave Technology, 2021, 39, 6334-6339.	4.6	22
103	Asymmetric transverse-load characteristics and polarization dependence of long-period fiber gratings written by a focused CO_2 laser. Applied Optics, 2007, 46, 3079.	2.1	21
104	Unique temperature sensing characteristics of CO2-laser-notched long-period fiber gratings. Optics and Lasers in Engineering, 2009, 47, 1044-1048.	3.8	21
105	Rough Side-Polished Fiber With Surface Scratches for Sensing Applications. IEEE Photonics Journal, 2015, 7, 1-7.	2.0	21
106	Highly sensitive torsion sensor based on directional coupling in twisted photonic crystal fiber. Applied Physics Express, 2018, 11, 042501.	2.4	21
107	Suppression of parasitic interference in a fiber-tip Fabry-Perot interferometer for high-pressure measurements. Optics Express, 2018, 26, 28178.	3.4	21
108	Highly sensitive gas refractive index sensor based on hollow-core photonic bandgap fiber. Optics Express, 2019, 27, 29649.	3.4	21

#	Article	IF	CITATIONS
109	Twist-direction-dependent orbital angular momentum generator based on inflation-assisted helical photonic crystal fiber. Optics Letters, 2019, 44, 459.	3.3	21
110	Broadband Thermo-Optic Switching Effect Based on Liquid Crystal Infiltrated Photonic Crystal Fibers. IEEE Photonics Journal, 2015, 7, 1-7.	2.0	20
111	Novel fabrication technique for phase-shifted fiber Bragg gratings using a variable-velocity scanning beam and a shielded phase mask. Optics Express, 2018, 26, 13311.	3.4	20
112	Bragg Gratings in Suspended-Core Photonic Microcells for High-Temperature Applications. Journal of Lightwave Technology, 2018, 36, 2920-2924.	4.6	20
113	Femtosecond Laser Microprinting of a Fiber Whispering Gallery Mode Resonator for Highly-Sensitive Temperature Measurements. Journal of Lightwave Technology, 2019, 37, 1241-1245.	4.6	20
114	Recent Progress in Fabrications and Applications of Heating-Induced Long Period Fiber Gratings. Sensors, 2019, 19, 4473.	3.8	19
115	In-Fiber Collimator-Based Fabry-Perot Interferometer with Enhanced Vibration Sensitivity. Sensors, 2019, 19, 435.	3.8	19
116	Highly sensitive hydrogen sensor based on an in-fiber Mach-Zehnder interferometer with polymer infiltration and Pt-loaded WO ₃ coating. Optics Express, 2021, 29, 4147.	3.4	19
117	Low short-wavelength loss fiber Bragg gratings inscribed in a small-core fiber by femtosecond laser point-by-point technology. Optics Letters, 2019, 44, 5121.	3.3	19
118	High-order OAM mode generation in a helical long-period fiber grating inscribed by an oxyhydrogen-flame. Optics Express, 2021, 29, 43371.	3.4	19
119	Gas Pressure Sensor Based on CO ₂ -Laser-Induced Long-Period Fiber Grating in Air-Core Photonic Bandgap Fiber. IEEE Photonics Journal, 2015, 7, 1-7.	2.0	18
120	Strain-based tunable optical microresonator with an in-fiber rectangular air bubble. Optics Letters, 2018, 43, 4077.	3.3	18
121	A ZnO nanowire-based microfiber coupler for all-optical photodetection applications. Nanoscale, 2019, 11, 8319-8326.	5.6	18
122	Shape Sensing Using Two Outer Cores of Multicore Fiber and Optical Frequency Domain Reflectometer. Journal of Lightwave Technology, 2021, 39, 6624-6630.	4.6	18
123	3D nanoprinted kinoform spiral zone plates on fiber facets for high-efficiency focused vortex beam generation. Optics Express, 2020, 28, 38127.	3.4	18
124	Design and realization of 3D printed fiber-tip microcantilever probes applied to hydrogen sensing. Light Advanced Manufacturing, 2022, 3, 1.	5.1	18
125	Bidirectional Bend Sensor Employing a Microfiber-Assisted U-Shaped Fabry-Perot Cavity. IEEE Photonics Journal, 2017, 9, 1-8.	2.0	17
126	Optical Fiber Tag Based on an Encoded Fiber Bragg Grating Fabricated by Femtosecond Laser. Journal of Lightwave Technology, 2020, 38, 1474-1479.	4.6	17

#	Article	IF	CITATIONS
127	Optical Fiber Integrated Functional Micro-/Nanostructure Induced by Two-Photon Polymerization. Frontiers in Materials, 2020, 7, .	2.4	17
128	Single-mode helical Bragg grating waveguide created in a multimode coreless fiber by femtosecond laser direct writing. Photonics Research, 2021, 9, 2052.	7.0	17
129	In-Fiber Polymer Microdisk Resonator and Its Sensing Applications of Temperature and Humidity. ACS Applied Materials & Interfaces, 2021, 13, 48119-48126.	8.0	17
130	High-Speed All-Optical Modulator Based on a Polymer Nanofiber Bragg Grating Printed by Femtosecond Laser. ACS Applied Materials & Interfaces, 2020, 12, 1465-1473.	8.0	16
131	Helical Long-Period Fiber Gratings as Wavelength-Tunable Orbital Angular Momentum Mode Generators. IEEE Photonics Technology Letters, 2020, 32, 418-421.	2.5	16
132	Helical Intermediate-Period Fiber Grating for Refractive Index Measurements With Low-Sensitive Temperature and Torsion Response. Journal of Lightwave Technology, 2021, 39, 6678-6685.	4.6	16
133	Slit Beam Shaping for Femtosecond Laser Point-by- Point Inscription of High-Quality Fiber Bragg Gratings. Journal of Lightwave Technology, 2021, 39, 5142-5148.	4.6	16
134	Unique Temperature Dependence of Selectively Liquid-Crystal-Filled Photonic Crystal Fibers. IEEE Photonics Technology Letters, 2016, 28, 1282-1285.	2.5	15
135	Hollow-Core-Fiber-Based Interferometer for High-Temperature Measurements. IEEE Photonics Journal, 2017, 9, 1-9.	2.0	15
136	Bragg gratings inscribed in selectively inflated photonic crystal fibers. Optics Express, 2017, 25, 28442.	3.4	15
137	Temperature-insensitive directional transverse load sensor based on dual side-hole fiber Bragg grating. Optics Express, 2021, 29, 17700.	3.4	15
138	Beat frequency tuning in dual-polarization distributed feedback fiber laser using side polishing technique. Optics Express, 2018, 26, 34699.	3.4	15
139	Intensity-modulated bend sensor by using a twin core fiber: theoretical and experimental studies. Optics Express, 2020, 28, 14850.	3.4	15
140	Fiber-interface directional coupler inscribed by femtosecond laser for refractive index measurements. Optics Express, 2020, 28, 14263.	3.4	15
141	Orthogonal long-period fiber grating for directly exciting the orbital angular momentum. Optics Express, 2020, 28, 27044.	3.4	15
142	Femtosecond laser line-by-line inscription of apodized fiber Bragg gratings. Optics Letters, 2021, 46, 5663.	3.3	15
143	Investigation of Long-Period Grating Resonances in Hollow-Core Photonic Bandgap Fibers. Journal of Lightwave Technology, 2011, 29, 1708-1714.	4.6	14
144	Highly birefringent suspended-core photonic microcells for refractive-index sensing. Applied Physics Letters, 2014, 105, 061105.	3.3	14

#	Article	IF	CITATIONS
145	Long Period Fiber Grating Inscribed in Hollow-Core Photonic Bandgap Fiber for Gas Pressure Sensing. IEEE Photonics Journal, 2017, 9, 1-7.	2.0	14
146	Dual-Polarization Distributed Feedback Fiber Laser Sensor Based on Femtosecond Laser-Inscribed In-Fiber Stressors for Simultaneous Strain and Temperature Measurements. IEEE Access, 2020, 8, 97823-97829.	4.2	14
147	Gas detection in a graphene based dual-mode fiber laser microcavity. Sensors and Actuators B: Chemical, 2021, 348, 130694.	7.8	14
148	Stabilized Ultra-High-Temperature Sensors Based on Inert Gas-Sealed Sapphire Fiber Bragg Gratings. ACS Applied Materials & Interfaces, 2022, 14, 12359-12366.	8.0	14
149	Bragg resonance in microfiber realized by two-photon polymerization. Optics Express, 2018, 26, 3732.	3.4	13
150	Highly Sensitive Temperature Sensor Based on All-Fiber Polarization Interference Filter With Vernier Effect. IEEE Access, 2020, 8, 207397-207403.	4.2	13
151	A Probe-Shaped Sensor With FBG and Fiber-Tip Bubble for Pressure and Temperature Sensing. Photonic Sensors, 2021, 11, 411-417.	5.0	13
152	High-sensitivity gas pressure sensor based on a multimode interferometer using hollow-core tube lattice fiber. Optics Letters, 2020, 45, 4571.	3.3	13
153	A Wearable Breath Sensor Based on Fiber-Tip Microcantilever. Biosensors, 2022, 12, 168.	4.7	13
154	Mode field profile and polarization dependence of long period fiber gratings written by CO2 laser. Optics Communications, 2008, 281, 2522-2525.	2.1	12
155	High-Sensitivity Gas Pressure Sensor Based on Fabry–Pérot Interferometer With a Side-Opened Channel in Hollow-Core Photonic Bandgap Fiber. IEEE Photonics Journal, 2015, 7, 1-7.	2.0	12
156	Ultrasensitive Temperature Sensor Based on a Fiber Fabry–Pérot Interferometer Created in a Mercury-Filled Silica Tube. IEEE Photonics Journal, 2015, 7, 1-9.	2.0	12
157	Sensing Characteristics of Tilted Long Period Fiber Gratings Inscribed by Infrared Femtosecond Laser. Sensors, 2018, 18, 3003.	3.8	12
158	Highly Reproducible, Isotropic Optofluidic Laser Based on Hollow Optical Fiber. IEEE Journal of Selected Topics in Quantum Electronics, 2019, 25, 1-6.	2.9	12
159	Recent advance in hollow-core fiber high-temperature and high-pressure sensing technology [Invited]. Chinese Optics Letters, 2021, 19, 070601.	2.9	12
160	High-sensitivity optical fiber temperature sensor based on a dual-loop optoelectronic oscillator with the Vernier effect. Optics Express, 2020, 28, 35264.	3.4	12
161	Sensitivity Enhancement for Fiber Bragg Grating Strain Sensing Based on Optoelectronic Oscillator With Vernier Effect. IEEE Photonics Journal, 2021, 13, 1-6.	2.0	12
162	Highly Sensitive Surface Plasmon Resonance Humidity Sensor Based on a Polyvinyl-Alcohol-Coated Polymer Optical Fiber. Biosensors, 2021, 11, 461.	4.7	12

#	Article	IF	CITATIONS
163	Femtosecond laser inscribed helical long period fiber grating for exciting orbital angular momentum. Optics Express, 2022, 30, 4402.	3.4	12
164	Polymer-Coated Hollow Fiber Optofluidic Laser for Refractive Index Sensing. Journal of Lightwave Technology, 2020, 38, 1550-1556.	4.6	11
165	Helical Long Period Fiber Grating Inscribed in Elliptical Core Polarization-Maintaining Fiber. IEEE Access, 2021, 9, 59378-59382.	4.2	11
166	Compact Surface Plasmon Resonance IgG Sensor Based on H-Shaped Optical Fiber. Biosensors, 2022, 12, 141.	4.7	11
167	Fabry-Perot Interferometer Based on a Fiber-Tip Fixed-Supported Bridge for Fast Glucose Concentration Measurement. Biosensors, 2022, 12, 391.	4.7	11
168	The Effect of 4-Octyldecyloxybenzoic Acid on Liquid-Crystalline Polyurethane Composites with Triple-Shape Memory and Self-Healing Properties. Materials, 2016, 9, 792.	2.9	10
169	Temperature Insensitivity Polarization-Controlled Orbital Angular Momentum Mode Converter Based on an LPFG Induced in Four-Mode Fiber. Sensors, 2018, 18, 1766.	3.8	10
170	Helicity Enhanced Torsion Sensor Based on Liquid Filled Twisted Photonic Crystal Fibers. Sensors, 2020, 20, 1490.	3.8	10
171	Ultrasensitive refractometer based on helical long-period fiber grating near the dispersion turning point. Optics Letters, 2022, 47, 2602.	3.3	10
172	Femtosecond laser 3D printed micro objective lens for ultrathin fiber endoscope. Fundamental Research, 2024, 4, 123-130.	3.3	10
173	Investigating Transverse Loading Characteristics of Microstructured Fiber Bragg Gratings With an Active Fiber Depolarizer. IEEE Photonics Technology Letters, 2009, 21, 1450-1452.	2.5	9
174	Long period fiber gratings written in photonic crystal fibers by use of CO2 laser. Photonic Sensors, 2013, 3, 193-201.	5.0	9
175	Side-Opened Suspended Core Fiber-Based Surface Plasmon Resonance Sensor. IEEE Sensors Journal, 2015, 15, 4086-4092.	4.7	9
176	Liquid-Crystal-Filled Side-hole Fiber for High-Sensitivity Temperature and Electric Field Measurement. Micromachines, 2019, 10, 761.	2.9	9
177	Self-Imaging Effect in Liquid-Filled Hollow-Core Capillary Waveguide for Sensing Applications. Sensors, 2020, 20, 135.	3.8	9
178	Super-Variable Focusing Vortex Beam Generators Based on Spiral Zone Plate Etched on Optical Fiber Facet. Journal of Lightwave Technology, 2021, 39, 1416-1422.	4.6	9
179	Effects of π-Bridge on Fused-Ring Electron Acceptor Dimers. ACS Applied Polymer Materials, 2021, 3, 23-29.	4.4	9
180	Excitation of high order orbital angular momentum modes in ultra-short chiral long period fiber gratings. Optics Express, 2021, 29, 39384.	3.4	9

#	Article	IF	CITATIONS
181	Distributed high-temperature sensing based on optical frequency domain reflectometry with a standard single-mode fiber. Optics Letters, 2022, 47, 882.	3.3	9
182	Influence of Side-Polished Fiber Surface Topography on Surface Plasmon Resonance Wavelengths and the Full Width at Half-Maximum. IEEE Photonics Journal, 2017, 9, 1-13.	2.0	8
183	Red Shift of Side-Polished Fiber Surface Plasmon Resonance Sensors With Silver Coating and Inhibition by Gold Plating. IEEE Photonics Journal, 2017, 9, 1-13.	2.0	8
184	High-Sensitivity Detection of IgC Operating near the Dispersion Turning Point in Tapered Two-Mode Fibers. Micromachines, 2020, 11, 270.	2.9	8
185	Effects of linking units on fused-ring electron acceptor dimers. Journal of Materials Chemistry A, 2020, 8, 13735-13741.	10.3	8
186	ZnO Microwire-Based Fiber-Tip Fabry-Pérot Interferometer for Deep Ultraviolet Sensing. Journal of Lightwave Technology, 2021, 39, 4225-4229.	4.6	8
187	Highly Localized Point-by-Point Fiber Bragg Grating for Multi-Parameter Measurement. Journal of Lightwave Technology, 2021, 39, 6686-6690.	4.6	8
188	A Fabry–Perot Interferometer With Asymmetrical Tapered-Fiber for Improving Strain Sensitivity. Journal of Lightwave Technology, 2021, 39, 1509-1514.	4.6	8
189	High purity optical vortex generation in a fiber Bragg grating inscribed by a femtosecond laser. Optics Letters, 2020, 45, 6679.	3.3	8
190	High-Spatial-Resolution High-Temperature Sensor Based on Ultra-Short Fiber Bragg Gratings With Dual-Wavelength Differential Detection. Journal of Lightwave Technology, 2022, 40, 2166-2172.	4.6	8
191	Torsion-tunable OAM mode generator based on oxyhydrogen-flame fabricated helical long-period fiber grating. Optics Express, 2022, 30, 21085.	3.4	8
192	Fabrication of Long-Period Gratings by Femtosecond Laser-Induced Filling of Air-Holes in Photonic Crystal Fibers. IEEE Photonics Technology Letters, 2010, , .	2.5	7
193	Solid Optical Fiber With Tunable Bandgaps Based on Curable Polymer Infiltrated Photonic Crystal Fiber. Journal of Lightwave Technology, 2016, 34, 5616-5619.	4.6	7
194	Femtosecond Laser Microprinting of a Polymer Optical Fiber Interferometer for High-Sensitivity Temperature Measurement. Polymers, 2018, 10, 1192.	4.5	7
195	Symmetric Step-Apodized Distributed Feedback Fiber Laser With Improved Efficiency. IEEE Photonics Journal, 2019, 11, 1-11.	2.0	7
196	Orbital angular momentum generator based on hollow-core photonic bandgap fiber grating. Applied Physics Express, 2019, 12, 072004.	2.4	7
197	High-Precise Fractional Orbital Angular Momentum Probing With a Fiber Grating Tip. Journal of Lightwave Technology, 2021, 39, 1867-1872.	4.6	7
198	All-Dielectric Phase-Gradient Metasurface Performing High-Efficiency Anomalous Transmission in the Near-Infrared Region. Nanoscale Research Letters, 2021, 16, 158.	5.7	7

#	Article	IF	CITATIONS
199	Room-Temperature Fiber Tip Nanoscale Optomechanical Bolometer. ACS Photonics, 2022, 9, 1586-1593.	6.6	7
200	Highly Sensitive Hydrogen Sensor Based on an Optical Driven Nanofilm Resonator. ACS Applied Materials & Interfaces, 2022, 14, 29357-29365.	8.0	7
201	Selective-Fluid-Filling Technique of Microstructured Optical Fibers. Journal of Lightwave Technology, 2010, , .	4.6	6
202	Long Period Fiber Gratings Inscribed With an Improved Two-Dimensional Scanning Technique. IEEE Photonics Journal, 2014, 6, 1-8.	2.0	6
203	The effect of liquid crystal fillers on structure and properties of liquid crystalline shape memory polyurethane composites II: 4-hexadecyloxybenzoic acid. Journal of Materials Science, 2017, 52, 2628-2641.	3.7	6
204	Growth dynamics of ZnO nanowire on a fiber-tip air bubble. Optical Materials Express, 2017, 7, 3433.	3.0	6
205	Taper Embedded Phase-Shifted Fiber Bragg Grating Fabricated by Femtosecond Laser Line-by-Line Inscription. IEEE Photonics Journal, 2018, 10, 1-8.	2.0	6
206	Nonlinear Hydraulic Pressure Response of an Improved Fiber Tip Interferometric High-Pressure Sensor. Sensors, 2020, 20, 2548.	3.8	6
207	All Fiber-Optic Immunosensors Based on Elliptical Core Helical Intermediate-Period Fiber Grating with Low-Sensitivity to Environmental Disturbances. Biosensors, 2022, 12, 99.	4.7	6
208	Polarimetric fiber laser for relative humidity sensing based on graphene oxide-coated D-shaped fiber and beat frequency demodulation. Optics Express, 2022, 30, 15998.	3.4	6
209	The impact of liquid crystal fillers on structure and properties of liquid-crystalline shape-memory polyurethane composites I: 4-dodecyloxybenzoic acid. Journal of Materials Science, 2016, 51, 10229-10244.	3.7	5
210	An All-Fiber Fan-Out Device for Varying Twin-Core Fiber Types. Journal of Lightwave Technology, 2017, 35, 5121-5126.	4.6	5
211	Antiresonant Reflecting Guidance and Mach-Zender Interference in Cascaded Hollow-Core Fibers for Multi-Parameter Sensing. Sensors, 2018, 18, 4140.	3.8	5
212	High-Efficiency Inscription of Fiber Bragg Grating Array with High-Energy Nanosecond-Pulsed Laser Talbot Interferometer. Sensors, 2020, 20, 4307.	3.8	5
213	Strain, torsion and refractive index sensors based on helical long period fibre grating inscribed in small-core fibre for structural condition monitoring. Advances in Structural Engineering, 2021, 24, 1248-1255.	2.4	5
214	Compact and broad wavelength range tunable orbital angular momentum mode generator based on cascaded helical photonic crystal fibers. Optics Letters, 2020, 45, 5032.	3.3	5
215	Multifunctional optoelectronic device based on liquid crystal selectively filled flat-plate photonic crystal fiber. Optik, 2022, 250, 168328.	2.9	5
216	A Nondestructive Measurement Method of Optical Fiber Young's Modulus Based on OFDR. Sensors, 2022, 22, 1450.	3.8	5

#	Article	IF	CITATIONS
217	Quasi-Distributed Temperature and Strain Sensors Based on Series-Integrated Fiber Bragg Gratings. Nanomaterials, 2022, 12, 1540.	4.1	5
218	Numerical analysis of an ultra-broadband and highly efficient beam splitter in the visible region. Optics Express, 2022, 30, 18032.	3.4	5
219	Transverse load, static strain, temperature and vibration measurement using a cascaded FBG/EFPI/LPFG sensor system. , 0, , .		4
220	Determination of Optical Fiber Parameters Based On Fiber Gratings and a Search Procedure. Journal of Lightwave Technology, 2017, 35, 3591-3596.	4.6	4
221	A High-Strength Strain Sensor Based on a Reshaped Micro-Air-Cavity. Sensors, 2020, 20, 4530.	3.8	4
222	A Twin-Core and Dual-Hole Fiber Design and Fabrication. Journal of Lightwave Technology, 2021, 39, 4028-4033.	4.6	4
223	A Multi-Parameter Integrated Sensor Based on Selectively Filled D-Shaped Photonic Crystal Fiber. Materials, 2022, 15, 2811.	2.9	4
224	Slit Beam Shaping for Femtosecond Laser Point-by-Point Inscription of Highly Localized Fiber Bragg Grating. Journal of Lightwave Technology, 2022, 40, 5722-5728.	4.6	4
225	Fiber Bragg gratings in small-core Ge-Doped photonic crystal fibers. , 2008, , .		3
226	Highly sensitive temperature sensor based on a Mach-Zehnder interferometer created in graded index fiber. , 2018, , .		3
227	Hollow-Core Fiber-Tip Interferometric High-Temperature Sensor Operating at 1100 °C with High Linearity. Micromachines, 2021, 12, 234.	2.9	3
228	Post-treatment techniques for enhancing mode-coupling in long period fiber gratings induced by CO2 laser. Photonic Sensors, 2015, 5, 339-344.	5.0	2
229	Ultrasensitive magnetic field sensor based on in-fiber Mach-Zehnder interferometer and magnetic fluid. , 2016, , .		2
230	Femtosecond laser micromachining of microfluidic fiber sensors. , 2016, , .		2
231	Enhanced surface plasmon resonance fiber sensor based on Graphene Oxide. , 2018, , .		2
232	Sensitivity-enhanced Temperature Sensor Based on Cascaded Polymer-infiltrated Mach-Zehnder Interferometers Created in Graded Index Fibers. , 2019, , .		2
233	Fiber Bragg Grating with Enhanced Cladding Modes Inscribed by Femtosecond Laser and a Phase Mask. Sensors, 2020, 20, 7004.	3.8	2
234	Shape sensing using two outer cores of multi-core fiber based on OFDR. , 2022, , .		2

#	Article	IF	CITATIONS
235	Direct generation of orbital angular momentum in orthogonal fiber Bragg grating. Optics Express, 2022, 30, 28745.	3.4	2
236	Correction to "Exact Analytical Solution for Raman Fiber Laser". IEEE Photonics Technology Letters, 2008, 20, 458-458.	2.5	1
237	UV-laser-inscribed fiber Bragg gratings in photonic crystal fibers and sensing applications. Proceedings of SPIE, 2011, , .	0.8	1
238	Improved arc discharge technique for inscribing compact long period fiber gratings. Proceedings of SPIE, 2014, , .	0.8	1
239	High-sensitivity strain sensors based on in-fiber reshaped air bubbles. Proceedings of SPIE, 2015, , .	0.8	1
240	High-sensitivity gas pressure sensors based on in-fiber devices. Proceedings of SPIE, 2015, , .	0.8	1
241	Graphene oxide modified surface plasmon resonance sensor based on side-polished fiber. Proceedings of SPIE, 2017, , .	0.8	1
242	Gas pressure sensing based on antiresonant reflecting guidance hollow-core fiber. Proceedings of SPIE, 2017, , .	0.8	1
243	Photonic crystal fiber with selective infiltration for high sensitivity simultaneous temperature and strain measurement. , 2017, , .		1
244	Twin-core few-mode fiber Bragg gratings inscribed by femtosecond laser. , 2017, , .		1
245	Femtosecond-Laser-Inscribed Fiber Bragg Gratings for High-Tempertature Sensing. , 2018, , .		1
246	Sapphire Fiber Bragg Gratings with Improved Spectral Properties for High-temperature Measurements. , 2019, , .		1
247	A Surface Plasmon Resonance Sensor Based on D-Shaped All-Solid Photonic Crystal Fiber. , 2019, , .		1
248	Multicomponent Photonic Glass for Temperature Insensitive Fiber Probe. Journal of Lightwave Technology, 2020, 38, 4470-4477.	4.6	1
249	Fabrications and applications of fiber gratings based on microstructured optical fibers. Shenzhen Daxue Xuebao (Ligong Ban)/Journal of Shenzhen University Science and Engineering, 2013, 30, 23-29.	0.2	1
250	Inscription and improvement of novel fiber Bragg gratings by 800 nm femtosecond laser through a phase mask. , 2016, , .		1
251	Investigation of Side-Polished Panda Fibers for Strain Measurement and Surface Plasmon Resonance-Based Biochemical Sensing. , 2020, , .		1
252	Optical switch based on fluid-filled photonic crystal fiber. , 2009, , .		0

#	Article	IF	CITATIONS
253	Fluid-filled microstructured optical fibers and switching applications. Proceedings of SPIE, 2009, , .	0.8	Ο
254	Optical fiber gratings written in microstructured optical fibers. , 2012, , .		0
255	Post-processing techniques for enhancing mode-coupling in long period fiber gratings. , 2012, , .		О
256	Long period fiber gratings written in photonic crystal fibers by CO ₂ laser. Proceedings of SPIE, 2013, , .	0.8	0
257	Selective-fluid-filled photonic crystal fibers and applications. Proceedings of SPIE, 2013, , .	0.8	0
258	Ultrasensitive temperature sensor based on whispering gallery mode resonance in bent coated optical fiber loop. , 2014, , .		0
259	Tunable phase-shifted FBG based on an in-grating bubble. Proceedings of SPIE, 2014, , .	0.8	0
260	Gas pressure sensors based on in-fiber devices. , 2015, , .		0
261	Refractive index sensor based on side-polished fiber Bragg grating. , 2015, , .		0
262	Microstructured optical fiber devices for gas pressure measurements. , 2015, , .		0
263	High-sensitivity bend sensor based on Mach-Zehnder interferometer using photonic crystal fiber. , 2015, , .		0
264	CO <inf>2</inf> laser writing of long period fiber grating in air-core photonic bandgap fiber as gas pressure sensor. , 2015, , .		0
265	Ultrahigh-sensitivity temperature sensor based on in-fiber Fabry-Perot interferometer. , 2015, , .		0
266	A new fiber-tip Fabry-Perot interferometer and its application for pressure measurement. , 2015, , .		0
267	Phase-shifted gratings and negative-index gratings fabricated by 800 nm femtosecond laser overexposure. , 2016, , .		0
268	Fabrication and characterization of an egg-shaped hollow fiber microbubble. , 2017, , .		0
269	A novel fabrication method of fiber-tip Fabry-Perot interferometer for high-sensitivity gas-pressure measurements. , 2017, , .		0
270	Miniature Fabry-Perot interferometer strain sensor based on an elliptical air bubble. , 2017, , .		0

#	Article	IF	CITATIONS
271	Fabrication and characterization of a single-ended ultra-thin spherical microbubble. , 2017, , .		Ο
272	Multi-channel mode converters based on in-line fiber modal interferometer. , 2017, , .		0
273	Improving the refractive index sensitivity of long period fiber grating with coating ZnO thin film. , 2017, , .		0
274	Omnidirectional bending sensor based on fiber Bragg gratings inscribed in a seven-core fiber. , 2018, , .		0
275	Highly sensitive bend measurements using a miniature fiber collimator-based Fabry-Perot Interferometer. , 2018, , .		Ο
276	Undamaged Measurement of the Sub-Micron Diaphragm and Gap by Tri-Beam Interference. Journal of Lightwave Technology, 2019, 37, 5840-5847.	4.6	0
277	Femtosecond Laser-inscribed Multimode Fiber Bragg Gratings. , 2019, , .		0
278	Femtosecond Laser-Inscribed Ultra-Weak Fiber Bragg Grating Array for Distributed High-Temperature Measurements. , 2021, , .		0
279	Multicore Fiber Bragg Gratings Array Shape Sensor Fabricated with an Auto-Alignment Femtosecond Laser Point-by-Point Technology. , 2021, , .		0
280	Encapsulated Sapphire Fiber Bragg Grating Sensor with Improved High-Temperature Performance. , 2021, , .		0
281	Silt-Beam Shaping Method for Femtosecond Laser Point-by-Point Inscription of Highly Localized Fiber Bragg Gratings with Enhanced Cladding Modes. , 2021, , .		0
282	Optical attenuators based on fluid-filled photonic crystal fibers. , 2013, , .		0
283	Microstructured Optical Fiber Devices for Gas Pressure Measurements. , 2015, , .		Ο
284	Refractive index sensing with long period grating in thin-core-fiber. , 2016, , .		0
285	Polarization-dependent phase-shifted fiber Bragg gratings inscribed by femtosecond laser overexposure. , 2016, , .		0
286	A new method to fabricate phase-shifted Fiber Bragg gratings by femtosecond laser point-by-point inscription. , 2016, , .		0
287	A Gas Pressure Sensor Based on Long Period Grating Inscribed in Air-core Photonic Bandgap Fiber. , 2016, , .		0
288	Fabrication of phase-shifted fiber Bragg gratings with a velocity-changed scanning UV laser beam. , 2017, , .		0

#	Article	IF	CITATIONS
289	Fiber surface Bragg grating waveguide fabricated by femtosecond laser micromachining. , 2017, , .		Ο
290	Ultrafast laser-induced negative-index fiber Bragg gratings with enhanced thermal stability. Proceedings of SPIE, 2017, , .	0.8	0
291	Fabrication of side-polished fiber Bragg grating for refractive index sensor. , 2018, , .		0
292	CO2-Laser-Inscribed Long Period Fiber Gratings: From Fabrication to Applications. , 2019, , 1379-1423.		0
293	CO2-Laser-Inscribed Long Period Fiber Gratings: From Fabrication to Applications. , 2019, , 1-45.		0
294	Ultrafast laser inscription of fiber Bragg gratings with low polarization dependent loss. , 2020, , .		0
295	Gas pressure sensor based on a hollow cavity modulated phase shifted fiber Bragg grating. , 2021, , .		0
296	Optical microresonator based on an in-fiber rectangular air bubble. , 2021, , .		0
297	Polymer-Filled In-Fiber Mach-Zehnder Interferometer with Pt-loaded WO3 Coating for Trace Hydrogen Detection. , 2020, , .		0
298	Highly birefringent fiber grating laser sensors based on femtosecond laser-inscribed in-fiber stressors. , 2020, , .		0
299	Fiber-tip polymer microcantilever for hydrogen sensing. , 2020, , .		0
300	Large-Scale Multiplexed in-Fiber Micro-Cavity Array for Distributed High Temperature Sensing. , 2021, , .		0
301	Orbital Angular Momentum Mode Sensing Technology Based on Intensity Interrogation. Sensors, 2022, 22, 1810.	3.8	Ο